EXPERIMENTAL HEAT AND MASS TRANSFER STUDIES ON HORIZONTAL FALLING FILM ABSORBER USING WATER-LITHIUM BROMIDE

Arshi Banu PS, [1,2*], Sudharsan NM[2]

[*1]Dept of Mechanical Engineering, Hindustan Institute of Technology and Science, Chennai, India.

[2]Dept of Mechanical Engineering, Rajalakshmi Engineering College, Anna University, Chennai, India.

[*]Corresponding author; E-mail: psarshib@hindustanuniv.ac.in, arshi.banu@gmail.com.

Abstract

Vapour absorption systems are more viable technology option in energy and environmental perspective in cooling and heating applications. Among the four major components of vapour absorption system, the absorber plays a vital role in deciding the performance, size and cost. Horizontal falling film absorbers comparatively contain good heat and mass transfer characteristics than other type of absorbers for working fluids such as water-lithium bromide. Literature shows that experimental approach of performance evaluation of absorber is more realistic and accurate than the theoretical approach. Hence in the present work, a detail experimental study has been done on horizontal tube falling film absorber using water-lithium bromide as a working fluid. The set up consists of two major components viz. absorber and generator. Absorber contains three columns of tubes, with eight rows in each column. Detailed parametric study has been done by considering influence of spray density, cooling water flow rate, cooling water temperature and concentration on solution temperatures, cooling water temperatures, inlet and outlet concentrations, heat flux, mass flux, heat transfer coefficient and mass transfer coefficient with the help of plots. Results have been validated and literature gaps have been discussed.

Key words*: solar; vapour absorption refrigeration/cooling system; absorber; horizontal falling film; spray density; heat flux; mass flux; heat transfer coefficient; mass transfer coefficient;*

1. Introduction

Vapour absorption systems is an ecofriendly technology, as it utilizes solar heat energy and natural materials as working fluids [1]. Among the four major components, absorber performance playes vital role in deciding the overall system performance, size and cost. In systems that employ H_2O-LiBr as working fluid, horizontal falling-film absorbers are more favourable due to their good heat and mass transfer characteristics [2].

Theoretical models of performance of horizontal falling film absorbers using H_2O-LiBr [3] based on certain assumptions such as the physical properties of the solution are constant and independent of temperature and concentration, vapor pressure equilibrium exists between the vapor and liquid phase, the flow is laminar and non-wavy throughout to name a few. In fact, many of such

factors significantly influence the absorption performance and hence the results of such model deviate significantly from the experimental results. Hence experimental approach in the study of heat and mass transfer characteristics in an absorber is superior to analytical approach [4].

Various experimental works on horizontal falling film absorbers using H_2O-LiBr as working fluid are available in literature which are described through review works [4, 5].They are categorized based on tube geometry, tube surface and additive influence on performance enhancement of the absorber. Several researchers have performed parametric performance study on horizontal falling film absorber [3, 6, 8 – 17]. There is paucity of experimental works that describe the influence of each parameter in enhancing the heat and mass transfer performance of the absorber.

In the present work, a detailed experimental parametric study was carried out on the heat and mass transfer characteristics of a horizontal falling film absorber using H_2O-LiBr as working fluid. Apart from heat and mass transfer coefficients, inlet and outlet solution temperatures behavior, inlet and outlet cooling water temperature behavior, inlet and outlet concentration behavior and heat and mass flux behavior are studied. The influence of spray densities, cooling water flow rate, cooling water temperature and concentration of lithium bromide on above parameters are discussed with the plots.

2. Description of experimental setup and working

The line diagram of the experimental set-up used in the present study is shown in Figure 1. It consists of two major components of vapour absorption refrigeration system, namely, the absorber and the generator. Absorber is horizontal drum contains copper tube bundle with 8 rows and 3 columns. Tube bundle specifications are given in detail in the Table 1. A distribution tray with the equidistant holes of diameter 2.6 mm in three rows has been placed exactly above the tube bundle. The absorber has two glass windows, one to illuminate the absorber and the other is to visualize the flow pattern of strong solution over tubes. Generator is a horizontal drum with 20 liters of capacity. It has three flow circuits: the solution circuit, the vapor circuit and the coolant circuit.

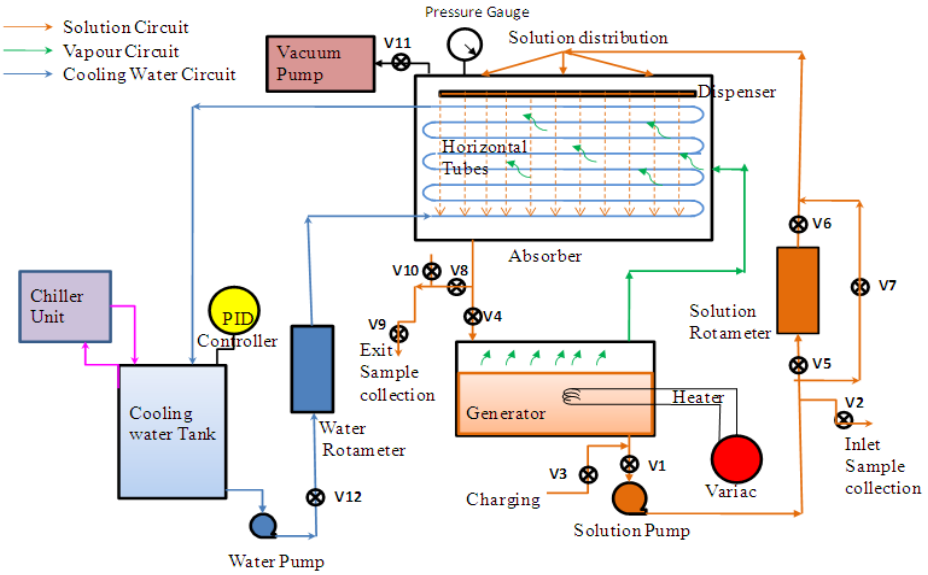

Figure 1: Line diagram of experiental setup of horizontal falling film absorber

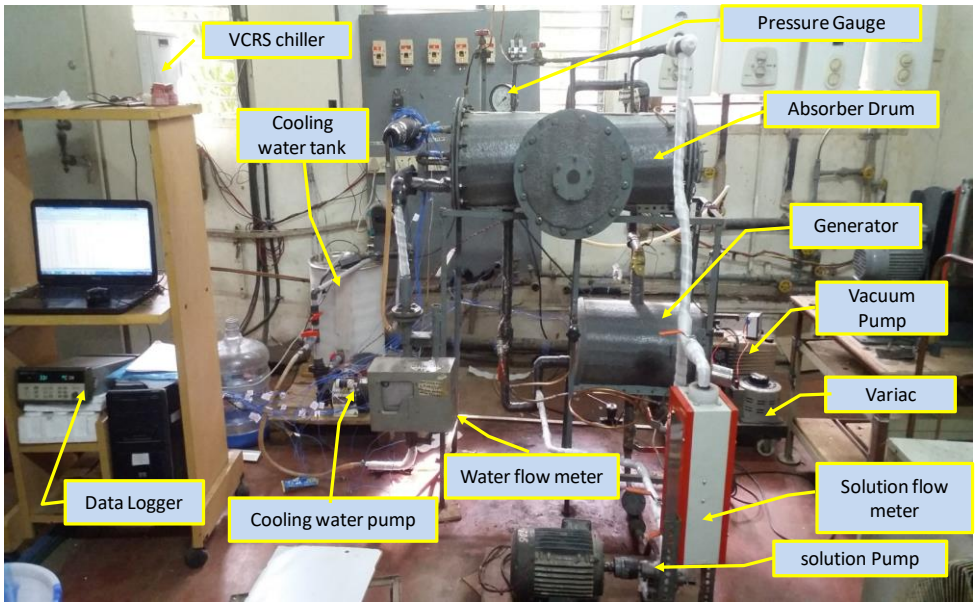

Figure 2: Pictorial view of experimental setup of horizontal falling film absorber

Number of tubes (n)	8 Rows X 3 Columns=24
Outer diameter (d_o)	12.70 mm
Inner diameter (d_i)	10.92 mm
Spacing(S)	12.70 mm
Pitch to dia ratio	2
Length (L)	70 cm

Table 1: Tube bundle specification

2.1. Solution Circuit

Generator has been charged with H_2O-LiBr solution to required quantity and concentration through valve 3. Solution has been heated by electric heater, connected through Variac to vary the required amount of heat load. On heating of H_2O-LiBr solution generates water vapour and resulting strong solution leaves at the bottom of the generator. A solution gear pump is used to pump the strong solution from generator to the top of the absorber through three ports situated above the distributer tray. The solution from distributer tray is sprayed over the first row of tube bundle after wetting the first row it flow to consecutive tubes. Weak solution formed in absorber due to absorption is carried back to the generator through 25.4 mm diameter pipe for recirculation. Solution flowrate is measured using glass type Rotameter with teflan coated float. In this circuit, the solution temperature at inlet of the absorber, exit of the absorber and at the exit of each tube in the bundle is measured using T type (copper-constantan) thermocouples. Valve 2 and valve 8 are arranged to divert the required amount of strong and weak solution to measure the density using Pycnometer, respectively.

2.2. Vapor circuit

While heat is being added to the generator by the heater, water vapour boils out of the solution flows to the absorber through a vapour inlet situated in the middle of absorber drum across the tube bundle. The water vapor is absorbed at the interface of the solution film which finally leaves at the

bottom of the absorber as a weak solution through valve 4. In this circuit, the temperature of the vapor is measured at the exit of the generator and at inlet of absorber.

2.3. Coolant circuit

In this circuit, a cooling water pump is used to circulate the water between coolant tank and absorber tube bundle. The coolant enters at the bottom row of the tube bundle in the absorber via a common header. It flows through the copper tubes in a serpentine path and leaves at the top row of the bundle to another header. The coolant that leaves at the exit of the header is returned back to the coolant tank for recirculation. Cooling coils of vapour compression refrigeration system are inserted in coolant tank in order to reduce the heat load carries away from absorber. Constant temperature in cooling water tank is maintained by PID controller. The volume flow rate of the coolant is measured with the help of a metal tube rotameter before it enters into the absorber. In this circuit, the coolant temperature is measured at inlet, middle and top row of the tubes in the bundle. Details of instruments used during experiment their accuracy and error has been shown in Table 2. Pictorial view of entire experimental setup is shown in Figure 2.

Parameter	Instrument	Range/Max capacity	Accuracy	Minimum measured value	Error
Temperature	T-type copper-constantan thermocouples	-	0.5 °C	20 °C	2.5%
Pressure	Bourdon vaccume gauge	100kPa	0.5 %	1kPa	1.48%
Water flow rate	Metal type Rotameter	60-600 LPH	0.60%	180 LPH	2%
Solution flow rate	Glass type Rotameter	1-20LPM	1%	6 LPM	3.33%
Density	Pycnometer	50 ml	1%	50ml	02%
Heat input	Resistance		0.1 ohm	18 ohm	0.55%
	voltage		0.1V	95.3 V	0.11%
	Power		8.95W	500 W	1.79%

Table 1: Instrumentation-Accuracy-Error

3. Data Processing:[11, 14]

Overall heat transfer coefficient(U):

Logarithmic mean temperature difference(LMTD) is expressed as:

$$LMTD = ((T_{si} - T_{co}) - (T_{so} - T_{ci}))/ln[(T_{si} - T_{co})/(T_{so} - T_{ci})] \quad (1)$$

Heat transfer rate from cooling water to outside tube surface wall

$$Q = m_c C_{pc}(T_{co} - T_{ci}) = UA_o LMTD \quad (2)$$

Where heat transfer area of outside tube surface is

$$A_0 = n(\pi d_o L) \quad (3)$$

Heat transfer coefficient cooling water side(h_i):

Convective heat transfer coefficient of cooling water inside the tubes is given by Dittus-Boelter correlation

$$Nu_c = 0.023\, Re_c^{0.8}\ Pr_c^{0.4} = (h_i\, d_i)/k_c \quad (4)$$

Where cooling water Reynolds number is expressed as

$$Re_c = (u_c d_i)/\nu_c \quad (5)$$

Heat transfer coefficient solution side (h_o):

The heat transfer coefficient for the solution flowing outside the tubes

$$h_o = 1/((1/U - d_o/(d_i\, h_i\,)) \quad (6)$$

Mass transfer coefficient (h_m):

Mass flow rate of the solution per unit length/ Spray density

$$\Gamma_s = m_{si}/2nL \quad (7)$$

Where solution film Reynolds number is expressed as

$$Re_s = (4\Gamma_s)/\mu_s \quad (8)$$

The mass flow rate of the vapor absorbed in the absorption process

$$m_v = m_{si}\,(X_i/X_o - 1) \quad (9)$$

is obtained by the mass conservation of LiBr solution

The logarithmic mean concentration difference(LMCD) is expressed as

$$LMCD = ((X_{si} - X_i) - (X_{so} - X_o))/ln[(X_{si} - X_i)/(X_{so} - X_o)] \quad (10)$$

Where X_{si} and X_{so} are concentration calculated from the inlet and outlet absorber bulk solution temperature satisfying the vapor pressure equilibrium condition, respectively.

The mass transfer coefficient is expressed as

$$h_m = m_v/(\rho_s A_o\, LMCD\,) \quad (11)$$

Parameter	Min	Max
Spay density (Γ)	0.01 kg/m.s	0.05 kg/m.s
Cooling water flow rate (m_c)	0.07 kg/s(250 LPH)	0.14 kg/s(500 LPH)
Cooling water temperature(t_{ci})	25 ^{0}C	35 ^{O}C
Concentration (X_i)	55 %	60 %
Generator Heat load (Q_g)	1 kW	
Absorber Pressure(p_a)	1 kPa	

Table 2: Parameters range/values considered during experiment

4. Results and discussion

Parameter range considered during experiment is shown in Table 3. Results obtained from the calculations using equations (1) to (11) are discussed in this section. Input parameters considered for plotting are Spray density(solution flow rate), cooling water flow rate, cooling water temperature and concentration of LiBr solution. Influence of each input parameter on Solution inlet and outlet temperatures, cooling water inlet and outlet temperatures, solution concentrations at inlet and outlet, heat and mass flux and heat and mass transfer coefficient has been discussed in each sub sections.

4.1 Effect of Spray density (Γ):

Figure. 3(a-e) shows the influence of spray density (solution flow rate per length and per side) on various output parameters. Spray density range is considered from 0.01 to 0.05 kg/m.s(6-20 lpm) during these plots. Parameters kept at constant value are: mass flow rate of cooling water(m_c) as 0.11 kg/s (400 lph), cooling water temperature(t_{ci}) as 30°C, concentration of solution as 60%, heat load given to generator as 1 kW and absorber pressure as 1 kPa.

Variation of inlet solution (strong solution) temperature (t_{si}) and exit solution (weak solution) temperatures (t_{so}) with spray density are plotted in the Figure 3(a). Increase in solution flow over the horizontal tubes causes increase in exposed wet surface area which will enhance the absorption rate

and absorption heat. Hence it is observed that both the inlet and outlet solution temperatures increase with increase in spray density. With the increase in heat of absorption of the solution, heat carried away by the cooling water will also increase. Hence cooling water temperature will increase with spray density as shown in Figure 3(b). Figure 3(c) represents the variation of outlet solution concentration of absorber with spray density. With increase in spray density, absorption rate increases hence solution concentrations increases at constant absorber pressure. Figure 3(d) shows the influence of spray density on heat and mass fluxes. Increase in exposed interface area with increase in flow rate of solution will enhance the absorption capacity of water vapour in solution this will tend to increase in heat of absorption. Hence heat and mass flux increases with increase in spray density. Graphically it is expressed as; decrease in difference between solution concentrations and increase in solution flow rates (Figure 3(c)) will increase the mass flux. It is also observed that increase in difference between cooling water temperatures (Figure 3(b)) will increase the heat flux at constant cooling water flow rates. Figure 3(e) depicts the variation of heat and mass transfer coefficients with spray density. Increment in heat flux as well as decrement in log mean temperature difference(LMTD) causes to increase in heat transfer coefficient with spay density. Similarly increment in mass flux as well as decrement of log mean concentration difference (LMCD) promoting increment in mass transfer coefficient with spray density.

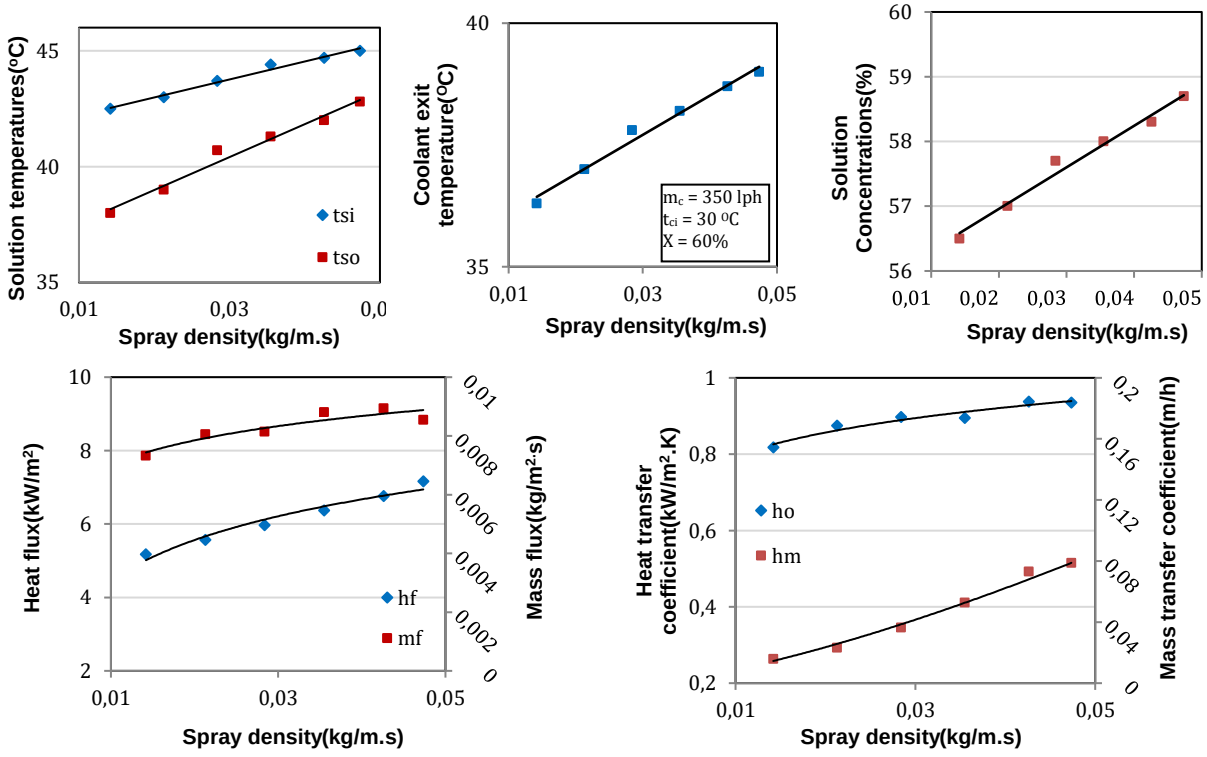

Figure 3: Effect of spray density on (a) Solution temperature (b) Coolant temperature (c) Solution concentration (d) Heat and mass flux (e) Heat and mass transfer coefficients

4.2 Effect of cooling water flow rate (m_c)

Figure 4 (a-e) shows the influence of cooling water flow rate(m_c) on various parameters. Cooling water flow rate varied from 0.07 to 0.14 kg/s(250 to 500 lph) in these plots. Parameters kept at constant value are: mass flow rate of solution/ Spray density(Γ) as 0.035 kg/m.s(at 15 lpm), cooling

water temperature(t_{ci}) as 30°C, concentration of solution as 60%, heat load given to generator as 1 kW and absorber pressure as 1 kPa.

The effect of mass flow rate of coolant on inlet and outlet solution temperatures in the absorber is shown in Figure 4(a). Higher velocities of cooling water tend to carry away more heat from solution which will reduce inlet and outlet solution temperatures with increase in cooling water flow rate. Figure 4(b) shows the variation of outlet cooling water temperature with mass flow rate of coolant. Reduction in solution temperatures causes lesser amount of heat rejection to the cooling water, hence cooling water temperatures also decreases with increase in cooling water flow rate. Figure 4(c) shows the variation of outlet concentrations of solution with coolant temperatures. Reduction of solution temperatures indirectly represents the decrease in corresponding solution concentrations with increase in coolant temperature. Figure 4(d) represents the variation of heat and mass fluxes with mass flow rate of the coolant. Heat of absorption is removed at higher rate by cooling water which will tend to increase the heat flux. Increase in absorption capacity will tend to increase the mass flux with increase in mass flow rate of cooling water. It can also describes graphically that increase in difference between solution concentrations (Figure 4(c)) at constant solution flow will increase the mass flux. Though there is decrease in difference between cooling water temperatures (Figure 4(b)), higher rate of mass flow rate of cooling water will increase the heat flux. Figure 4(e) presents the variation of heat and mass transfer coefficients with mass flow rate of the coolant. increament in heat and mass fluxes as well as decreament in corresponding LMTD and LMCD values will increase the heat and mass transfer coefficients with cooling water flow rate.

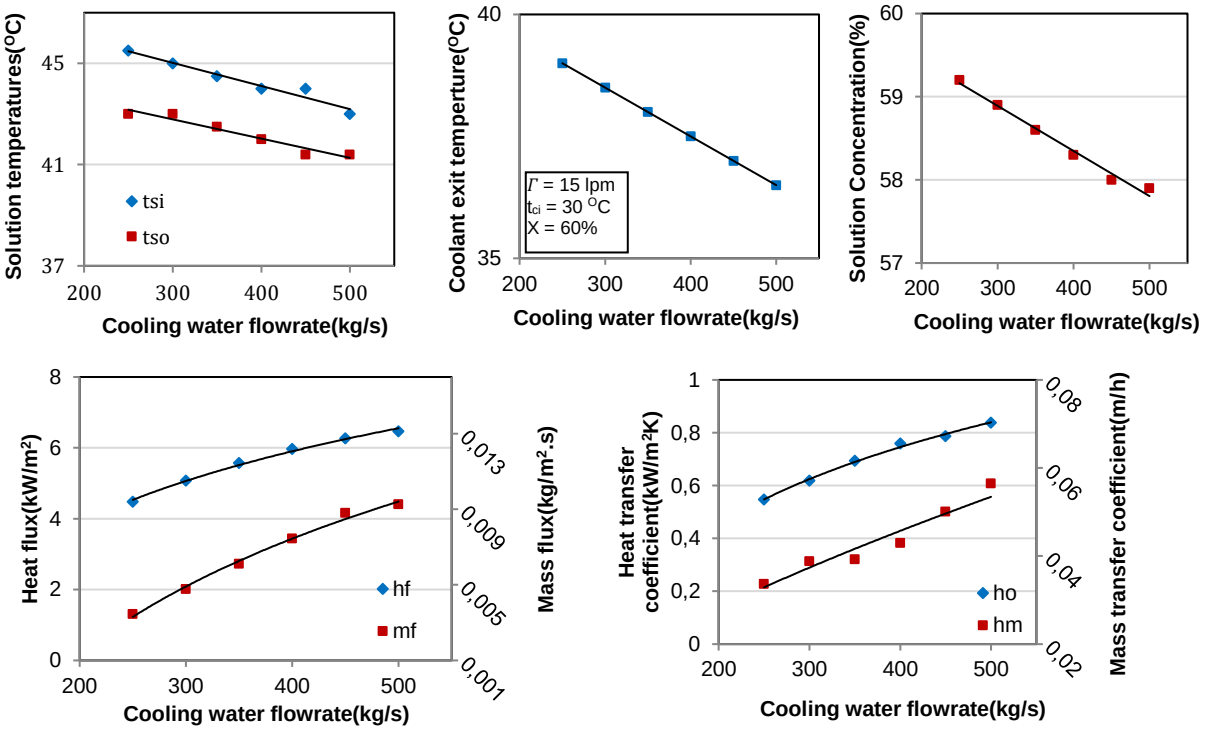

Figure 4: Effect of cooling water flow rate on (a) Solution temperatures (b) Coolant temperature (c) Solution concentration (d) Heat and mass flux (e) Heat and mass transfer coefficients

4.3 Effect of cooling water temperature (t_c):

Figure 5(a-e) depicts the variation of various parameters with inlet cooling water temperature(t_{ci}). Cooling water temperature varied from 25^{O}C to 30^{O}C. During the plots the parameters kept at constant value are: mass flow rate of solution/ Spray density(Γ) as 0.035 kg/m.s, cooling water flow rate(m_c) as 0.11 kg/s, concentration of solution as 60%, heat load given to generator as 1 kW and absorber pressure as 1 kPa.

Figure 5(a) shows the effect of inlet cooling water temperature on inlet and outlet solution temperatures. Figure 5(b) shows the effect of inlet cooling water temperature on outlet cooling water temperature. With increase in inlet cooling water temperature, heat rejection capacity decreases from solution to cooling water. Hence the solution temperatures as well as cooling water outlet temperatures show the increasing trend with increase in inlet cooling water temperatures. Reduction in absorption of water vapour will cause increment in outlet solution concentrations as shown in Figure 5(c). Figure 5(d) shows the heat and mass flux variation with cooling water temperatures. Due to reduction in absorption capacity and absorption heat both the heat and mass flux decreases with increase in inlet cooling water temperature. Graphically it is described as, decrease in difference between inlet and outlet coolant temperatures reduces the heat flux. Decrease in difference between inlet and outlet concentrations at constant solution flow rate reduces the mass flux with increase in inlet cooling water temperatures. Figure 5(e) presents the variation of heat and mass transfer coefficients with cooling water temperature.

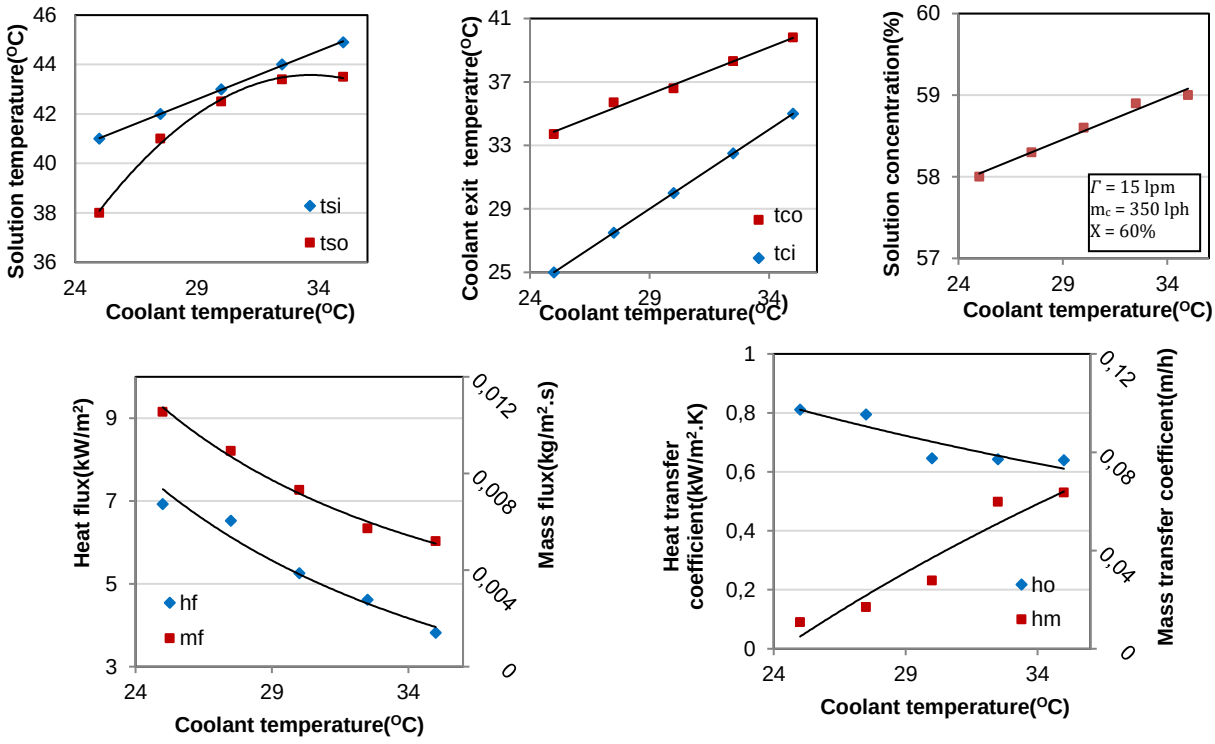

Figure 5: Effect of cooling water temperature on (a) Solution temperature (b) Coolant temperature (c) Solution concentration (d) Heat and mass flux (e) Heat and mass transfer coefficients

4.4 Effect of concentration(X):

Figure 6(a-e) represents the variation of various output parameters with concentration of solution. Concentration of LiBr solution is varied from 56% to 60% during the plots. The parameters

kept at constant values are: mass flow rate of solution/ Spray density(Γ) as 0.035 kg/m.s, cooling water flow rate(m_c) as 0.11 kg/s, cooling water temperature(t_{ci}) as 30^{O}C, heat load given to generator as 1 kW and pressure as 1 kPa. The variation of inlet and outlet solution temperatures with concentration of H_2O-LiBr solution is shown in Figure 6(a). With increase in percentage of lithium bromide salt in solution higher amount of heat of absorption is liberated. Hence higher solution temperatures are obtained with increase in solution concentrations.

Figure 6(b) shows the variation of outlet cooling water temperature with increase in solution concentration. Due to increase in heat loads cooling water temperatures also increases with increase in concentrations. Figure 6(c) shows the variation of inlet and outlet solution concentration with variation of solution concentration. Figure 6(d) presents the effect of H_2O-LiBr solution concentration on heat and mass fluxes. Absorption capacity of water vapour in the solution will increases with increase in lithium bromide content in solution hence mass flux will increase. With increase in absorption rate heat of absorption will also increases which will tend to increase the heat flux. It can be explained graphically as increase in difference between solution concentration represents the increase in mass flux. Increase in difference in cooling water temperatures represents the increase in heat flux with increase in concentrations.

Figure 6(e) shows the influence of solution concentration on heat and mass transfer coefficients. With the increase in solution concentration of H_2O-LiBr solution from 56% to 60%, the heat and mass transfer coefficients will increases. Increment in heat and mass fluxes and reduction in corresponding LMTD and LMCD values will causes the increment in heat and mass transfer coefficients.

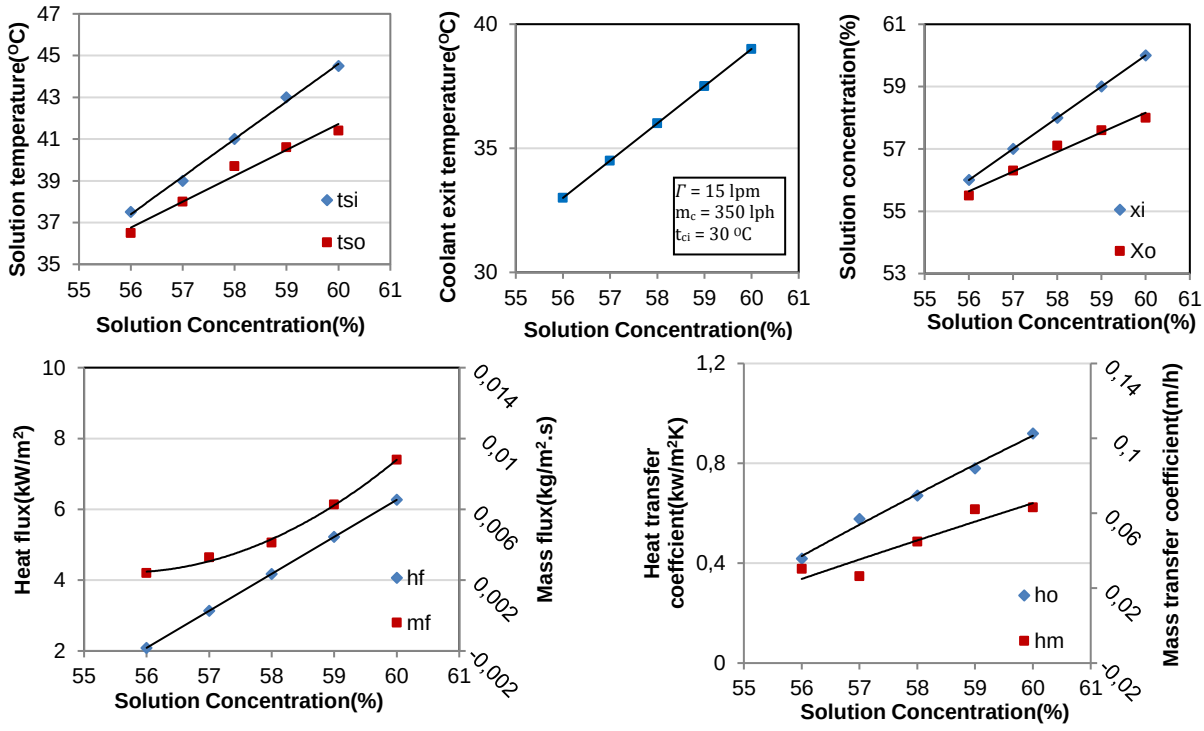

Figure 6: Effect Solution Concentration on (a) Solution temperature (b) Coolant temperature (c) Solution concentration (d) Heat and mass flux (e) Heat and mass transfer coefficients

5. Validation

Table 4 contains the literature works classified based on three parameters behavior; spray density, coolant flow rate and coolant temperature. Influnce of these parameters and corresponding heat transfer and mass transfer coefficient and heat and mass flux and their range are tabulated. Present experimental results are validated with literature. Most of the results published in the literature have discussed the influence of spray density on heat transfer coefficient and mass transfer coefficient. A few have discussed about the influence of coolant flow rate and coolant temperature. Heat and mass flux ranges also available in very few works in all the cases. Table 5 shows the heat transfer coefficient variation at different concentration of lithium bromide and validated with present study. Apart from above parameter present work has also focused in detail about solution temperatures, cooling water temperatures and solution concentrations in all cases where as it is rarely available in literature.

Author	Parameter	Range	Concentration (%)	HeatTrans Coefficient(kW/m^2.K)	Mass Trans Coefficient (m/h)	Heat Flux (kW/m^2)	MassFlux (kg/m^2.s)
Yoon[11]	**Spray density range(Kg/s.m)**	0.014-0.03	61	570-800	0.08-0.118	6.1-8.35	0.00215-0.00248
Islam [12]		0.03-0.059	60.4	_	_	_	0.00212-0.00217
Kyung[10]		0.0135-0.048	60	750-1150	_	_	_
Deng-ma[4]		0.01-0.05	63	1250-1800		_	3.2-8.8X10^{-5}
Haffman[7]		0.0074-0.044	56	300-800			
Present study		0.014-0.047	60	863-935	0.016-0.0787	5.17-7.16	0.0073-0.0085
Islam[12]	**Coolant flow rate(Kg/s)**	0.0632-0.088	60.4	_	_		0.00212-0.0021219
Yoon[11]		0.8-1.6	61	_	_	7.2-8.75	0.00218-0.0025
Present study		0.07-0.14	60	550-840	0.033-0.056	4.48-6.47	0.0035-0.0093
Islam[8]	**Coolant temperature (^{O}C)**	29.3-35.2	60.4	1440-1700	0.0218-0.026	_	_
Islam[12]		25-35	60.4	_	_	_	0.00219-0.00212
Present study		25-35	60	810 – 640	0.01-0.063	6.92-3.2	0.009-0.005

Table 3 Validation of Spray density, Coolant flow rate and temperature

Author	Concentration (%)	Spraydensity range(Kg/s.m)		Heat Transfer range Coefficient (kW/m^2.K)	
Deng-Ma[4]	60.1	0.0125	0.048	750	1400
	61.1	0.015	0.05	1200	1800
	63.7	0.0175	0.05	1700	3100
Haffman[7]	45.9	0.006	0.04	1150	1500
	51.2	0.006	0.0425	740	1050
	57	0.006	0.045	200	600
Kyung[10]	57	0.01	0.049	533	1000
	60	0.012	0.049	700	1100
Present Study	56	0.014	0.047	417.8	
	57	0.014	0.047	577.1	
	58	0.014	0.047	670.9	
	59	0.014	0.047	779.4	
	60	0.014	0.047	919.4	

Table 4 Validation of heat transfer coefficient at different concentrations

6. Conclusions

Experimental investigation has been done on horizontal falling film absorber and generator setup using water-lithium bromide solution as working fluid pair. Detailed heat and mass transfer behavior has been studies from parametric performance perspective. Following conclusions have been drawn from the study:

Increase in exposed interface area with increase in flow rate of solution will enhance the absorption capacity of water vapour in solution this will tend to increase in heat and mass flux and also heat and mass transfer coefficients. Higher removal rate of heat of absorption at higher cooling water flow rates will increase the heat flux and heat transfer coefficient. Increase in absorption capacity will increase in mass flux and mass transfer coefficient with increase in mass flow rate of cooling water. Due to reduction in heat load to cooling water, heat absorption capacity and vapour absorption capacity will get reduced with increase in cooling water inlet temperature. Hence both the heat and mass flux and heat transfer coefficient will decrease with cooling water temperature. Increase in lithium bromide content increases the absorption capacity of water vapour in solution results in increase in mass flux and mass transfer coefficient. With increase in heat of absorption heat flux and heat transfer coefficient will also increases with increase in lithium bromide concentration.

It is observed from the graphs that heat flux proportional to distance between inlet and outlet cooling water temperature curves and the cooling water flow rate. Mass flux increases with increase in difference between solution concentrations and solution flow rate. In all the cases solution curves have similar proportional behavior with the solution temperatures. Hence mass flux indirectly depends on distance between solution temperatures curves. Mass flux and mass transfer coefficient are not influenced by cooling water temperature. Heat and mass transfer coefficients behavior is not always similar to heat and mass flux behavior, it also equally depends on log mean temperature difference and log mean solution difference respectively. Mass transfer coefficient is more sensitive to outlet solution temperature and concentration than inlet temperature and concentration. Not all parameters have been dealt with and presented in the existing literature. In the present work the results have not only been validated but also the lacunae in the existing literature have now been incorporated for all the cases and addressed from the point of parametric performance.

Nomenclature

Γ	Spay density	h_f	Heat flux
t_{ci} /T_{ci}	Cooling water temperature at inlet	m_f	Mass flux
t_{co} /T_{co}	Cooling water temperature at outlet	h_o	Heat transfer coefficient
m_c	Mass flow rate of cooling water	h_m	Mass transfer coefficient
t_{si}/T_{si}	Solution temperature at inlet	Pr_c	Cooling water
t_{so}/T_{so}	Solution temperature at outlet	k_c	Tube thermal conductivity
X_i	Solution concentration at inlet	u_c	Cooling water velocity
X_o	Solution concentration at outlet	ν_c	Cooling water kinematic viscosity
m_{si}	Solution flow rate at inlet	μ_s	Solution dynamic viscosity

References

[1] Arshi Banu, P.S., Sudharsan, N.M., Review of water based vapour absorption cooling systems using thermodynamic analysis. *Renew. Sustain. Energy Rev*, 82(2017), pp. 3750–3761.

[2] Killion, J.D., Garimella, S., A Review of Experimental Investigations of Absorption of Wator Vapor in Liquid Films Falling Over Horizontal Tubes, *HVAC&R Research, 9* (2003), 2, pp. 111-136.
[3] Jeong, S., Garimella, S., Falling-film and Droplet Mode Heat and Mass Transfer in a Horizontal Tube Absorber, *International Journal of Heat and Mass Transfer, 45* (2002), 7, pp. 1445-1458.
[4] Deng, S.M., Ma, W.B., Experimental studies on the characteristics of an absorber using LiBr/H_2O solution as working fluid, *International Journal of Refrigeration, 22* (1999), pp. 293–301.
[5] Ibarra-Bahena, J., Romero, R.J., Performance of Different Experimental Absorber Designs in Absorption Heat Pump Cycle Technologies: A Review, *Energies, 7* (2014), pp.751-766.
[6] Cord,T., Andrea, L., Experimental Investigations on Falling-Film Absorbers with Horizontal Tubes – A Review, *International Refrigeration and Air Conditioning Conference*, (2012). Paper 1193.
[7] Beutler, A., Hoffmann, L., Ziegler, F., Alefeld, G., Gommed, K., Grossmann, G., Shavit, A., Experimental Investigation of Heat and Mass Transfer in Film Absorption on Horizontal and Vertical Tubes, Ab-Sorption 96, *International Absorption Heat Pump Conference*, Montreal, Canada, 1996, pp. 409-419.
[8] Islam, M., Wijeysundera, N.E., Ho, J.C., Evaluation of Heat and Mass Transfer Coefficients for Falling Film Tubular Absorbers, *Int J Refrigeration 26* (2003), 2, pp. 197-204.
[9] Soto Frances, V.M., Pinazo Ojer, J.M., Validation of a model for the absorption process of H_2O(vap) by a LiBr(aq) in a horizontal tube bundle, using a multi-factorial analysis, *International Journal of Heat and Mass Transfer, 46* (2003), pp.3299–3312.
[10] Kyung, I.S., Herold, K.E., Kang, Y.T., Experimental Verification of H_2O/LiBr Absorber Bundle Performance with Smooth Horizontal Tubes, *Int J Refrigeration, 30* (2007), 4, pp. 582-590.
[11] Yoon, J.I., Phan, T.T., Moon, C.G., Lee, H.S., Jeong, S. K., Heat and mass transfer characteristics of a horizontal tube falling film absorber with small diameter tubes, *Heat Mass Transfer, 44* (2008), 4, pp.437-444.
[12] Islam, M.R., Absorption process of a falling film on a tubular absorber: Experimental and numerical study, *Applied Thermal Engineering, 28* (2008), 11-12, pp.1386-1394.
[13] Bredow, D., Jain, P., Wohlfeil, A., Ziegler, F., Heat and Mass Transfer Characteristics of a Horizontal Tube Absorber in a Semi-Commercial Absorption Chiller, *Int J Refrigeration, 31* (2008), pp.1273-1281.
[14] Harikrishnan, L., Maiya, M.P., Tiwari, S., Investigations on Heat and Mass Transfer Characteristics of Falling Film Horizontal Tubular Absorber, *Int J Heat Mass Trans, 54* (2011), 11-12, pp.2609-2617.
[15] Arshi Banu, P.S., Sudharsan, N.M., Feasibility studies of single-effect H_2O-LiBr+LiI+$LiNO_3$+LiCl vapour absorption cooling system for solar based applications. *J Chem Pharm Sci*, 12(2017), pp. 1–7.
[16] Sadia Siddiqa, Anwar Hossain, M., Aqsa, Heat And Mass Transfer Effects on Natural Convection Flow Along a Horizontal Triangular Wavy Surface,*Thermal Science*, 21(2017), 2, pp.977 - 987.
[17] Senthil Kumar Chandrasekaran, Krishnan Srinivasan, Experimental Studies on Heat Transfer Characteristics of SS304 Screen Mesh Wick Heat Pipe, *Thermal Science*, 21(2017), 2, pp. S497 - S502.